Journal of Power Sources 213 (2012) 296–303

Contents lists available at SciVerse ScienceDirect

Journal of Power Sources

journal homepage: www.elsevier.com/locate/jpowsour

Thermal modelling of Li-ion polymer battery for electric vehicle drive cycles

Salvio Chacko [a,b], Yongmann M. Chung [a,*]

[a] School of Engineering and Centre for Scientific Computing, University of Warwick, Coventry CV4 7AL, UK
[b] Tata Motors European Technical Centre Plc., Coventry, UK

ARTICLE INFO

Article history:
Received 16 November 2011
Received in revised form
2 April 2012
Accepted 10 April 2012
Available online 16 April 2012

Keywords:
Battery thermal management
Lithium-ion polymer battery
Electro-thermal model
Electric vehicle drive cycles
Finite volume method

ABSTRACT

Time-dependent, thermal behaviour of a lithium-ion (Li-ion) polymer cell has been modelled for electric vehicle (EV) drive cycles with a view to developing an effective battery thermal management system. The fully coupled, three-dimensional transient electro-thermal model has been implemented based on a finite volume method. To support the numerical study, a high energy density Li-ion polymer pouch cell was tested in a climatic chamber for electric load cycles consisting of various charge and discharge rates, and a good agreement was found between the model predictions and the experimental data. The cell-level thermal behaviour under stressful conditions such as high power draw and high ambient temperature was predicted with the model. A significant temperature increase was observed in the stressful condition, corresponding to a repeated acceleration and deceleration, indicating that an effective battery thermal management system would be required to maintain the optimal cell performance and also to achieve a full battery lifesapn.

© 2012 Elsevier B.V. All rights reserved.

1. Introduction

Lithium-ion (Li-ion) polymer batteries potentially have much higher energy density ($\sim$ 400 W h l^{-1}) compared to other battery technologies, and they are already replacing nickel-metal hydride (NiMH) batteries for portable devices such as laptop computers and smart phones, and also for hand-held devices in the power tool industry [1]. The high energy/power density of Li-ion batteries has also made them an attractive power source in electric vehicles (EV) and hybrid electric vehicle (HEV), as they can provide longer driving range and higher acceleration. A typical battery pack for the EV application is composed of a large number of cells to provide the required power, and the compactness of battery packs poses a challenge for effective thermal management [1,2].

The major obstacles to designing a scaled-up of Li-ion batteries for EV applications have been safety, performance and overall cell life. The safety issue concerns the thermal runaway of battery cell, and the prediction and prevention of the propagation of thermal runaway have been studied by many researchers. A Li-ion cell generates heat during both charge and discharge, and the heat generation in the battery can increase sharply leading to overheating under stressful conditions such as high power draw and high ambient temperature while overheating can also be caused by defects in individual cells. If the cells are not thermally managed, the thermal runaway propagates into an entire battery pack. Various battery thermal management systems have been developed for air- and liquid-cooling to prevent the thermal runaway propagation without over-designing the cooling system [3].

The battery cell temperature also affects the performance, reliability and lifespan. High battery cell temperature can cause a shortening of the lifespan of the Li-ion battery due to increased degradation of the battery cell. It was found that every degree of cell temperature rise reduces the lifespan of the Li-ion battery by approximately two months in an operating temperature range of 30–40 °C [4]. To achieve a full lifespan, the cell temperature difference should be kept below 5 °C [5,6] as large temperature non-uniformity in the battery pack affects adversely overall cell lifespan as well as available cell capacity [7–10]. Therefore, a battery thermal management system enabling effective temperature control becomes essential for safety, performance, reliability and overall cell life [2,11,12]. For better design of thermal management system, understanding the real time behaviour of Li-ion cells in vehicle operating conditions is critical, and modelling its thermal behaviour in various EV drive cycles can help to design such battery thermal management systems [1].

Most of the previous studies have modelled the Li-ion cell thermal behaviour separately for charge or discharge, and have not considered the combined effect of them, typically present in vehicle load conditions [13]. Accurate modelling of the electro-thermal behaviour of Li-ion cells for dynamic electric loading conditions is a key requirement to improve battery thermal management system. In this study, a three-dimensional, fully coupled electro-

* Corresponding author. Tel.: +44 24 7657 4367; fax: +44 24 7641 8922.
E-mail address: Y.M.Chung@warwick.ac.uk (Y.M. Chung).

0378-7753/$ – see front matter © 2012 Elsevier B.V. All rights reserved.
doi:10.1016/j.jpowsour.2012.04.015

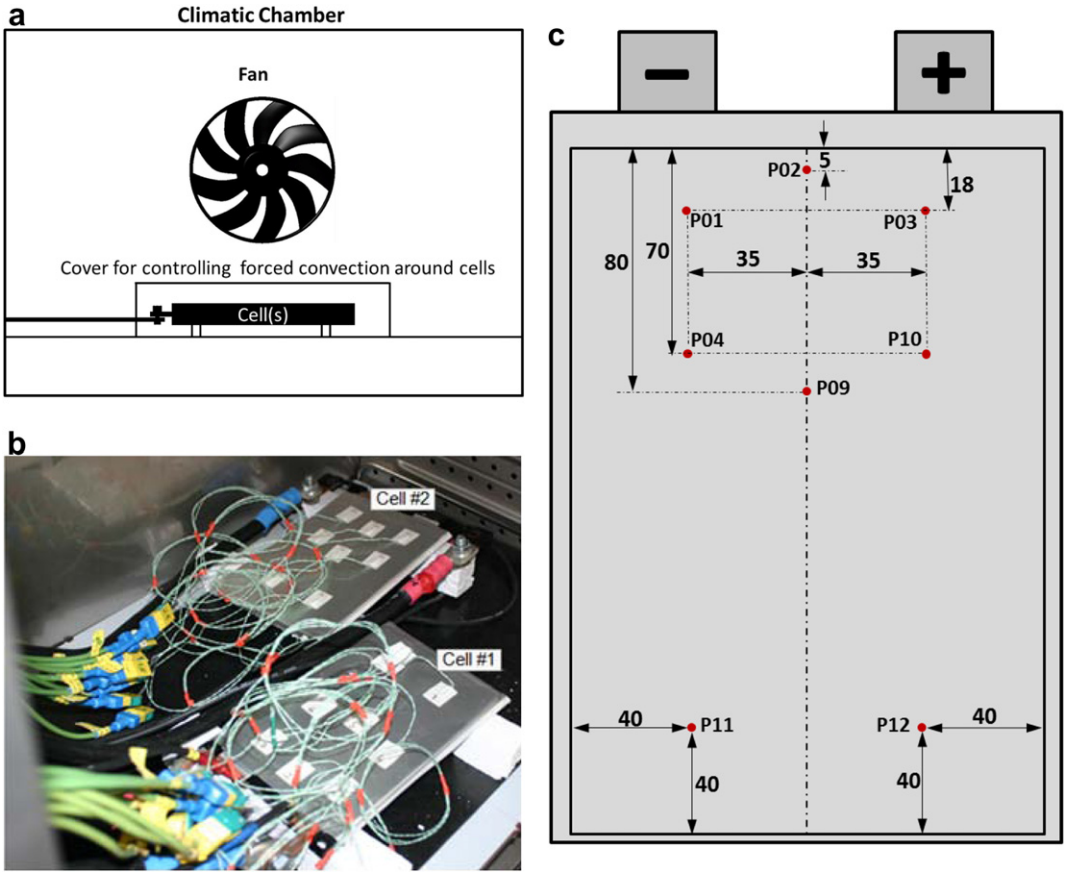

Fig. 1. a) Schematic of Li-ion cell test setup, b) instrumented cell in climatic chamber, and c) location of thermocouples in mm.

thermal cell model, which is capable of modelling vehicle load conditions, is developed. A high energy density Li-ion polymer pouch cell is tested at various charge and discharge rates to provide model characterisation data and also other relevant electrical and thermal data for validation. The current work focuses on electro-thermal modelling and its use in battery thermal management studies for EV/HEV applications. This model allows for scalability with accuracy and reasonable simulation time which is of prime importance while modelling full vehicle battery models.

2. Experimental setup

In this study, a high energy density Li-ion polymer pouch cell was tested to assess the electro-thermal cell model. The Li-ion cell has a graphite anode and a Li[NiMnCo]O_2 cathode with a nominal capacity of 20 A h. The schematic of the experimental setup is shown in Fig. 1. A climatic chamber was used to provide controlled thermal conditions during the test (Fig. 1 a). A box was installed around the cells to ensure well-defined free convective cooling and to protect the cells from forced convection, which would adversely affect the results. Fig. 1 b shows the Li-ion cells inside the box. The cell was prepared with 10 thermocouples to measure the temperature evolution on the cell surface during the test run. The locations of the thermocouples are shown in Fig. 1 c.

The Li-ion cell was tested using one of the Tata Motors European Technical Centre (TMETC) cell testing program within operating limits of the cell. The test cycle consisted of several constant current charge and discharge. Temperature was kept constant during the measurement at a reference temperature (T_{ref}). The electrical and thermal measurements at different reference temperatures and discharge rates were recorded. The cell was discharged at a constant discharge rate until the lower cut-off limit of 3 V was reached. Each discharge rate measurement required initialisation steps to precondition the cell before the measurement. These steps were to ensure that the prescribed electrical and thermal initial

Table 1
Cell test procedure. T_{test} is the test temperature.

Initialization step			
Temperature (°C)	Procedure	Value	Limit criteria
25	Discharge	1C	$U_{min} \leq 3.0$V
25	Break		10 min
25	Charge	1C	$U_{max} \geq 4.1$V $I_{min} \leq 1$A
Measurement step			
T_{test}	Break		≥ 40 min $T_{cell} = T_{test}$
T_{test}	Discharge	various C-rates	$U_{min} \leq 3.0$V
25	Break		30 min
25	Charge	IC	$U_{max} \geq 4.1$V $I_{min} \leq 1$A

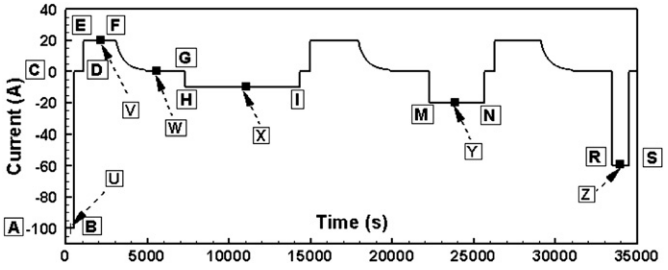

Fig. 2. Charge/discharge test cycle.

Table 2
Material properties used in the model. ρ is density, k is thermal conductivity, k_e is electrical conductivity, and c_p is specific heat.

	ρ [kg m^{-3}]	k [W mk^{-1}]	k_e [S mm^{-1}]	c_p [J kg^{-1} K^{-1}]
Pouch	1.15	0.16	0.1	1900
Positive Terminal	2.7	238	38300	900
Negative Terminal	8.36	398	63300	385

condition for each measurement was achieved. Table 1 shows the procedure for initialisation and measurement requirements in detail.

Fig. 2 shows the electric loading cycle. The section AB corresponds to a discharge current of 5C. The constant current discharge was followed by a 10 min break with no electric load. The remaining initialisation step before the next constant discharge consists of a 1C constant current charge (section EF) and a constant voltage section (section FG) where the current gradually reduces below 1 A. A 40 min break is then given for the relaxation processes in the cell chemistry before the next discharge rate measurement. This process of initialisation was performed between the discharge measurements: sections HI, MN and RS correspond to 0.5C, 1C, and 3C constant current discharge measurements, respectively. This whole process is repeated for different reference temperatures (T_{ref}), and thus providing the cell characterisation for various discharge rates and reference temperatures. The cell temperature and voltage during charge and discharge in the entire test cycle were recorded and compared with the the electro-thermal model prediction.

3. Coupled electro-thermal model

The Li-ion cell used in this study is comprised of a pouch case, electrode plates, electrolyte, and separators. To model the thermal behaviour of a battery cell accurately, the configuration, geometry, physical, chemical and electrochemical properties need to be known. In our electro-thermal model, the cell is characterised by a structure formed with a homogeneous layer, representing the anode, cathode and separator. The local heat generation in the battery cell due to the electrochemical reactions and the mass transfer of ions in the electrolyte are characterised by local internal resistance and the current densities. The performance of a cell is influenced by the charge/discharge rate, the ohmic resistance, the activation polarisation or charge transfer at the electrodes, the concentration polarisation in the electrolyte near the electrodes, and the cell temperature.

In this study, a three-dimensional mathematical model is used to predict the electrical and thermal performance of the Li-ion cell. The potential and current density distribution on the positive and negative electrodes are calculated using a PDE method proposed by Kwon *et al.* [14]. The charge conservation on the electrodes are modelled using a simplified polatisation characteristics of the electrodes, and Poisson equations for the potentials of the positive and negative electrodes (V_p and V_n) are derived in conjunction with Ohm's law. The cell terminal voltage can then be obtained as $V_{cell} = V_p - V_n$. A modified form of the polarisation expression proposed by Newman and Tiedemann [15] is used in this study to estimate the current density (J). An additional temperature dependency term is included in the polarisation expression to account for the Seebeck effect. In the following equation, the current density (J) is expressed as a function the cell terminal voltage (V_{cell}) and temperature:

$$J = Y\left(V_{cell} - U - b\left(T_i - T_{ref}\right)\right), \tag{1}$$

where Y is the conductance, and U is the equilibrium voltage. Y and U are estimated using the measurement data of V_{cell} and J. In the test, V_{cell} is measured as a function of depth-of-discharge (DOD), electric current and temperature. The first term on the right hand side is the Ohm's law term, and the current density is defined as $J = I/A$, where I is the current normal to the active material, and A is the active material area. The last term accounts for the Seebeck effect, where T_i is the cell temperature, and T_{ref} is the ambient temperature. The Seebeck coefficient b is to be determined from the test data.

The local heat generation rate of the Li-ion cell is then estimated during charge/discharge cycle based on the various losses in the cell [16]. The heat generation equation developed by Bernardi *et al.* [17] is used in this study:

$$Q = I\left(U - V_{cell} - T_i\frac{dU}{dT}\right), \tag{2}$$

where $I(U - V_{cell})$ estimates irreversible heat component due to deviation of cell voltage from the equilibrium voltage, and $I(T_i dU/dT)$ accounts for the reversible heat generation due to entropy change. dU/dT expresses the temperature dependence of the equilibrium voltage. The heat generation due to the ohmic resistance in the cell is also considered in the study [18]. Please note that the cell terminal voltage ($V_{cell} = V_p - V_n$) is obtained from the Poisson equations, as explained earlier.

In order to model the thermal behaviour of the Li-ion cell, the electrical model is combined with an energy balance. The unsteady three-dimensional heat conduction equation can be written as [19–21]:

$$\rho c_p\frac{\partial T}{\partial t} = \frac{\partial}{\partial x}\left(k_x\frac{\partial T}{\partial x}\right) + \frac{\partial}{\partial y}\left(k_y\frac{\partial T}{\partial y}\right) + \frac{\partial}{\partial z}\left(k_z\frac{\partial T}{\partial z}\right) + Q, \tag{3}$$

where ρ is the density, c_p the heat capacity, and k the effective thermal conductivity, and Q the heat generation in the Li-ion cell (Eq. (2)).

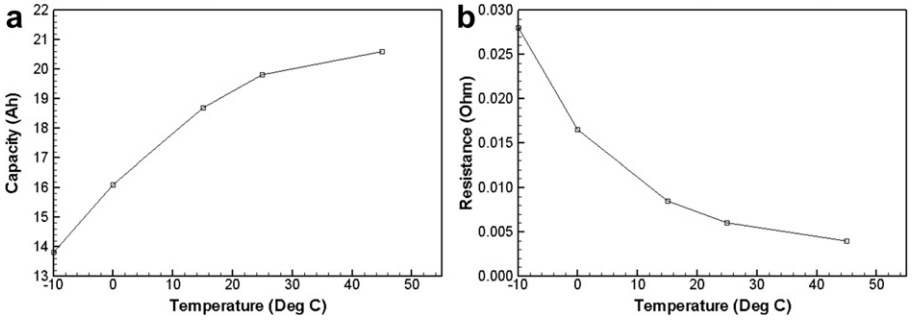

Fig. 3. Li-ion cell characteristics at several ambient temperatures. a) Capacity, and b) resistance variation with T_{ref}.

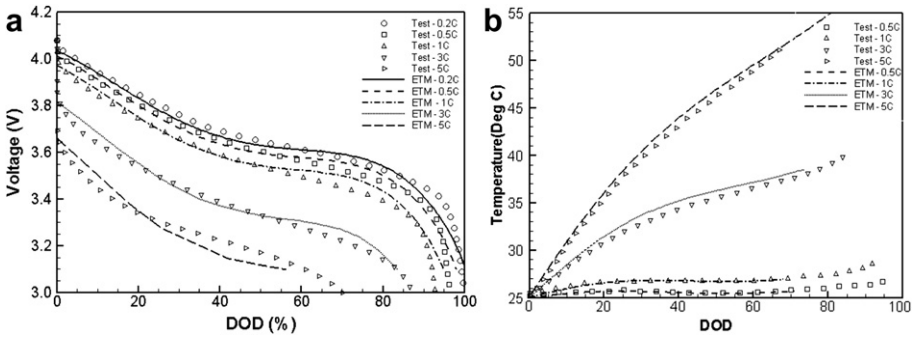

Fig. 4. Comparison of electro-thermal model prediction with experimental test results at $T_{ref} = 25\ ^{\circ}C$. a) Average voltage, and b) average temperature versus DOD at various discharge rates.

A convection thermal boundary condition is applied [17] at the cell surface, to consider the heat transfer (Q_c) with the environment,

$$Q_c = h\left(T - T_{ref}\right), \tag{4}$$

where $h = 25\ W\ m^{-2}K^{-1}$ is the convective heat transfer coefficient. The reference temperature is set to be $T_{ref} = 25\ ^{\circ}C$ to reflect the climatic chamber test temperature.

Eqs. (2) and (3) can predict the electro-thermal behaviour at every point in the Li-ion cell. The heat release from the cell, and subsequently the cell temperature are solved in both space and time. A three-dimensional finite volume method is used to solve the electro-thermal model, and the cell volume is discretised as a cartesian mesh in all three directions. In the finite volume model, the electrodes, separators and electrolyte are modelled at a macro level, and the volume-averaged material properties of all the cell components are used [21]. The enveloping pouch is also considered to model a realistic heat transfer to the environment. The material properties of the pouch and the tab used in the simulation are listed in Table 2. The density, thermal conductivity and heat capacity of the cell components are assumed to be uniform throughout the battery and to remain constant within a known range of temperature.

Y and U in Eqs. (1) and (2) are dependent on the depth-of-discharge (DOD) of the cell. Y and U values are estimated at various DOD using measurement data of cell voltage versus current density, where Y is the inverse of the slope, and U is the intercept. Then, their DOD dependency is modelled following Gu [22]. The conductance is given by:

$$Y(\mathrm{DOD}) = \sum_{k} a_k (\mathrm{DOD})^k \exp\left[\frac{E_{act}}{R}\left(\frac{1}{T_{ref}} - \frac{1}{T_i}\right)\right], \tag{5}$$

where R is the universal gas constant ($8.314\ J\ mol^{-1}\ K^{-1}$)). Arrhenius expression [23] is used to consider the temperature dependence of the electrochemical model property. The activation energy, E_{act}, is to be estimated from the test data. Similarly, the equilibrium voltage is given by

$$U(\mathrm{DOD}) = \sum_{m} b_m (\mathrm{DOD})^m, \tag{6}$$

where a_k and b_m are the fitting coefficients for Y and U, respectively. In this study, all fitting coefficients could represent up to 8th-order polynomials, and these coefficients are determined from discharge test data for various temperatures and C-rates. Similarly, dU/dT in Eq. (2) is also characterised with 8th-order polynomials.

Now, the values for b and E_{act} can be determined using discharge test data. From Eqs. (1), (5) and (6) we have

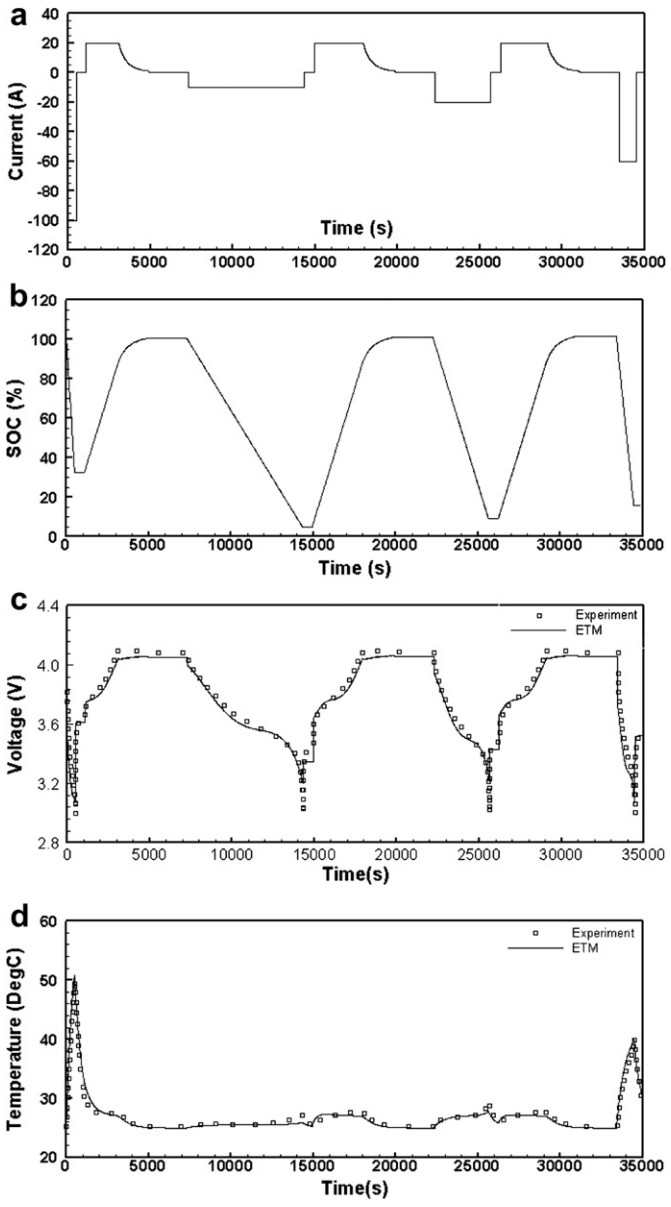

Fig. 5. Comparison of electro-thermal model prediction with experimental test results. a) Current, b) SOC, c) average voltage, and d) temperature at P01.

$$Y(\mathrm{DOD}, T_\mathrm{i}) = \sum_\mathrm{k} A_{\mathrm{k,i}}(\mathrm{DOD})^\mathrm{k} = \sum_\mathrm{k} a_\mathrm{k}(\mathrm{DOD})^\mathrm{k} \exp\left[\frac{E_\mathrm{act}}{R}\left(\frac{1}{T_\mathrm{ref}} - \frac{1}{T_\mathrm{i}}\right)\right], \quad (7)$$

$$U(\mathrm{DOD}) + b\left(T_\mathrm{i} - T_\mathrm{ref}\right) = \sum_\mathrm{m} B_{\mathrm{m,i}}(\mathrm{DOD})^\mathrm{m} = \sum_\mathrm{m} b_\mathrm{m}(\mathrm{DOD})^\mathrm{m} + b\left(T_\mathrm{i} - T_\mathrm{ref}\right), \quad (8)$$

where $A_{\mathrm{k,i}}$ and $B_{\mathrm{m,i}}$ are fitting coefficients for a given temperature T_i. From Eqs. (7) and (8), E_act and b can be deduced

$$\ln\left(\frac{\sum_\mathrm{k} A_{\mathrm{k,i}}(\mathrm{DOD})^\mathrm{k}}{\sum_\mathrm{k} a_\mathrm{k}(\mathrm{DOD})^\mathrm{k}}\right) = E_\mathrm{act}\left[\frac{1}{R}\left(\frac{1}{T_\mathrm{ref}} - \frac{1}{T_\mathrm{i}}\right)\right], \quad (9)$$

where E_act is the slope of the linear fitting of $\ln(\sum_\mathrm{k} A_{\mathrm{k,i}}(\mathrm{DOD})^\mathrm{k}/\sum_\mathrm{k} a_\mathrm{k}(\mathrm{DOD})^\mathrm{k})$ with respect to $1/R(1/T_\mathrm{ref} - 1/T_\mathrm{i})$, and b is the slope of the linear fitting of $(B_0 - b_0)$ to $(T_\mathrm{i} - T_\mathrm{ref})$. Test data at various temperatures, charge and discharge rates are used for cell parameter characterisation.

4. Results and discussion

Before describing the details of the electro-thermal model validation and prediction, key measured cell characteristics are summarised below. The change in cell capacity and resistance during discharge with a C-rate of 0.5C was measured at five different ambient temperatures (T_ref). Fig. 3 shows that the usable cell capacity increases significantly with T_ref while the internal resistance of the Li-ion cell decreases. The cell has the maximum usable capacity in a range of $25 \leq T_\mathrm{ref} \leq 45$ °C, where the internal resistance remains small.

4.1. Electro-thermal model validation

A three-dimensional transient electro-thermal model is used to predict unsteady temperature distribution on the Li-ion cell for a given electric load cycle and thermal boundary condition. The proposed electro-thermal model is correlated with test data for various discharge rates, and the DOD dependency of the electrical properties in Eqs. (5) and (6) are determined.

The electro-thermal model predictions are compared with experimental test results for several discharge rates. Fig. 4 shows the average cell voltage and temperature variation during discharge at $T_\mathrm{ref} = 25$ °C. The electrical behaviour prediction compares very well with the experimental test results over a wide range of DOD. The sudden voltage drop observed at the end of discharge (at high DOD) is correctly predicted in the model. The average cell temperature is also in good agreement with the test results. It can be seen that there is a steady increase in temperature during the constant current discharge. As the electrical load increases, the heat generation (given in Eq. (2)) and hence the cell temperature increase. As expected, the largest temperature rise occurs for the highest discharge rate (higher electrical load) due to the increased heat generation from the cell.

A Li-ion cell test cycle with a combination of various charge and discharge rates is then used for validation of charge and discharge

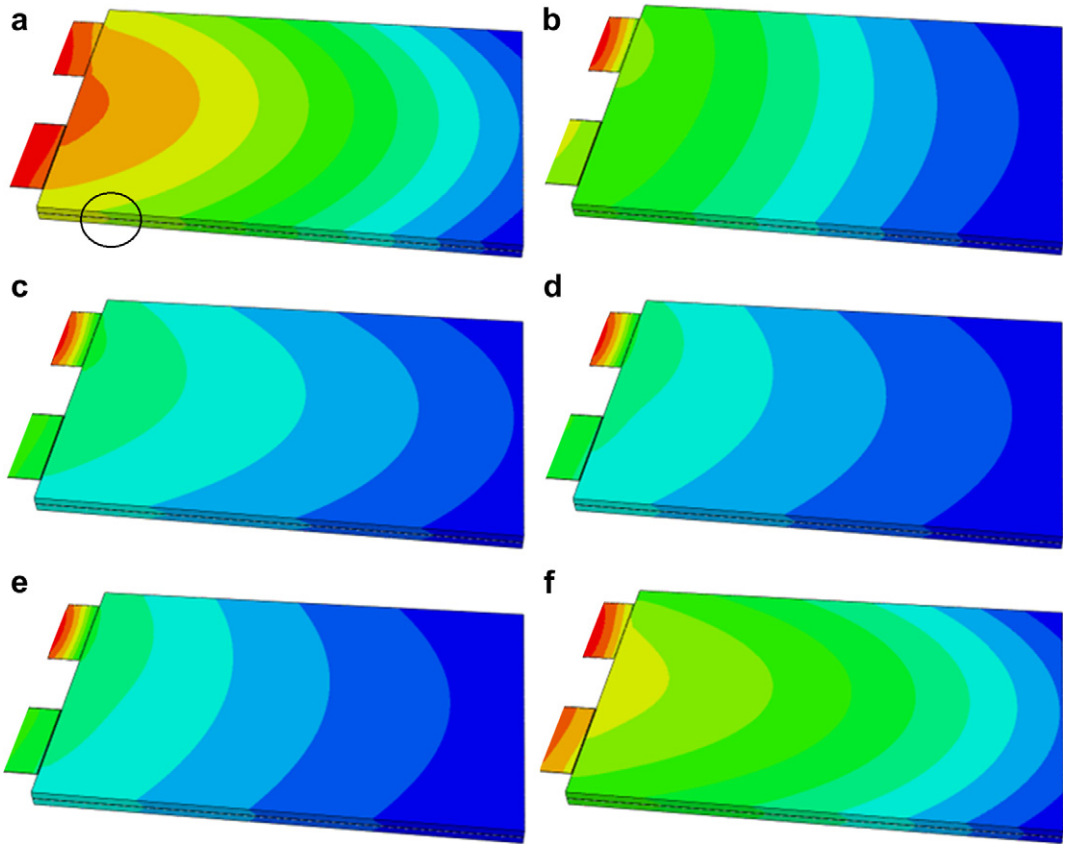

Fig. 6. Electro-thermal model temperature contour on cell face. A circle shows the temperature variation on the side wall. a) Point U: 5C discharge, b) Point V: 1C charge, c) Point W: constant voltage step, d) Point X: 0.5C discharge, e) Point Y: 1C discharge, and f) Point Z: 3C discharge.

behaviour modelling. Fig. 5 shows a comparison between the experimental test data and the electro-thermal model prediction. Various cell properties are gathered during the test, and the time variation of current, SOC, average cell voltage, and temperature are shown in the figure. A measuring point (P01) is located near the negative tab (see 1c). The overall electrical and thermal results from both test and electro-thermal model are in good agreement. The initial cell temperature is the same as the ambient temperature of $T_{ref} = 25$ °C. At the beginning of the cycle, the maximum applied discharge current of 5C causes a sharp increase in the cell temperature by more than 25 °C within approximately 7 min, and the amount of this temperature increase is correctly predicted in the model. The immediate voltage drop during the 5C discharge is also correctly captured. The voltage drop is followed by a relaxation phase with a sudden voltage rise. This is because the internal resistance decreases with the temperature rise due to faster kinetics, hence resulting in an increased cell voltage. Following the residual temperature build up from the 5C discharge and relaxation phase, the temperature remains below 30 °C during the charge. A similar trend of voltage and temperature response is also seen for an applied discharge current of 3C at the end of the cycle, and the instantaneous increase in temperature is about 15 °C. A modest temperature increase during 1C and 0.5C discharge is also well predicted in the model, displaying a much lower slope of the temperature history. As expected, SOC decreases linearly in time during constant current charge and decreases during discharge.

Fig. 6 shows the model prediction of temperature contours on the cell surface during the test cycle. Several phases in the test cycle are chosen to display the battery thermal characteristics during both charge and discharge. U, V, W, X, Y, and Z points during the test cycle are depicted in Fig. 2. Temperature on the positive terminal is higher than the negative terminal due to the lower electrical conductivity of the positive electrode as shown in Table 2. For higher discharge rates of 3C and 5C, the current flow is significantly high in the tab area due to an increased current density (in Eq. (1)), hence high temperature, particularly near the positive tab. The temperature variation on the cell progressively reduces for lower discharge rate as shown in the contour plot. The three-dimensional model is able to predict the temperature variation on the cell surface. A similar temperature variation on the tabs and cell were observed in the recent cell test thermal images of Kim *et al.* [18].

The results reported in this Section has provided a good validation for the current electro-thermal model. An excellent agreement is found between the Li-ion cell model prediction and the test data for charge and discharge, which clearly demonstrates the capability of the current Li-ion cell model to predict electro-thermal behaviour of the cell for different loading cycles.

4.2. Electro-thermal model prediction for vehicle operating conditions

The electro-thermal model is now applied to predict the Li-ion cell behaviour for vehicle operating conditions. Two vehicle operating conditions for the electro-thermal simulation are considered in this section. The first one (Cycle A) is the drive cycles during a hot environment test of an actual electric vehicle. From the TATA EV (prototype without cooling) hot environment tests at an proving ground during the summer, a gradual temperature increase was reported for 12% grade climb at 40 km h^{-1} [24]. It was also observed that at the end of the battery capacity there was a significant increase in battery temperature, indicating changes in internal resistance. The second one (Cycle B) is for a more severe test, where the vehicle was repeatedly accelerated from 20 km h^{-1} to 70 km h^{-1} and then braked back to 20 km h^{-1}. In this case, the battery temperature traces exhibited a small 'saw-tooth' effect of around 0.2–0.5 °C due to the transient peaks in the battery charge and discharge [24].

Fig. 7 shows the cell-level electro-thermal prediction for Cycle A. The simulation is performed for a constant discharge cycle of 1.2C (24 A), representing an electrical loading for a 40 km h^{-1}, 12% (ascending slope) climb vehicle operating condition. Fig. 7 shows the time variation of current, SOC, average cell voltage, and temperature on the cell surface for Cycle A. Three measuring points (P01, P03, and P10) are located near the negative tab (P01), and positive tab (P03 and P10). The SOC prediction shows that the cell would completely discharge in about 3000 s as would be expected for a cell of 20 A h nominal capacity. The temperature increases at the measuring points are gradual, and similar to the one observed in the vehicle level hot environment tests. The temperature rise time constant is approximately 300 s. There is an additional increase in the temperature at the end of discharge, which corresponds to an increased resistance.

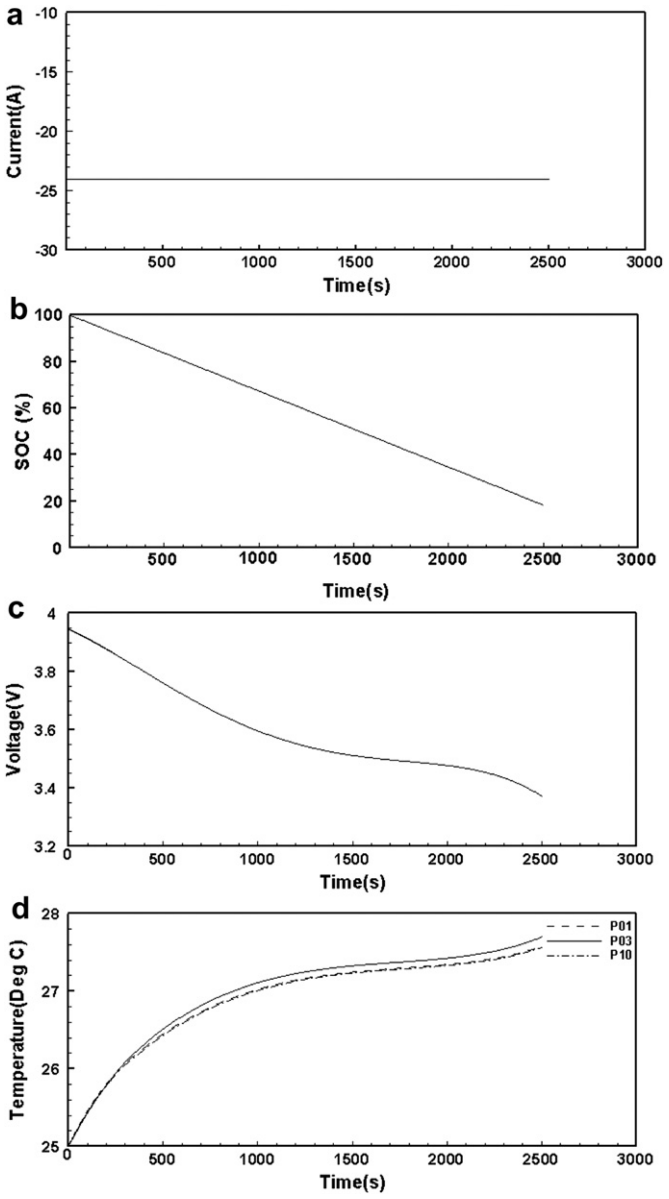

Fig. 7. Electro-thermal model prediction for a mild electric vehicle operating condition (Cycle A). a) Current, b) SOC, c) average voltage, and d) temperature at P01, P03 and P10.

The cell-level electro-thermal model is then applied to a more severe vehicle operating condition (Cycle B), where a vehicle is repeatedly accelerated and decelerated between 20 km h^{-1} and 70 km h^{-1}. Each cycle of 30 s is repeated for a total of 150 s to understand the accumulated thermal behaviour. The discharge step that represents acceleration was simulated for 1.7C (−34 A), and the charge step that represents braking was simulated for 0.83C (17 A). Fig. 8 shows the time variation of current, SOC, average cell voltage, and temperature at three measuring points (P01, P03, and P10) on the cell surface for Cycle B. A small saw-tooth effect is clearly seen in the cell temperature response at the charge/discharge transients, and a similar feature was observed on TATA EV (prototype without cooling) during the vehicle level hot environment tests [24]. It is found that the temperature increases by more than 1 °C during a aggressive cycle of 150 s at a modest ambient temperature. This would mean a substantial temperature increase for a standard 1 h aggressive hot environment test. Considering the fact that optimum Li-ion cell performance is found at around 25 °C cell operating point (see Fig. 3), this would mean that for such aggressive drive cycles the cells would potentially need an optimum active temperature control [2].

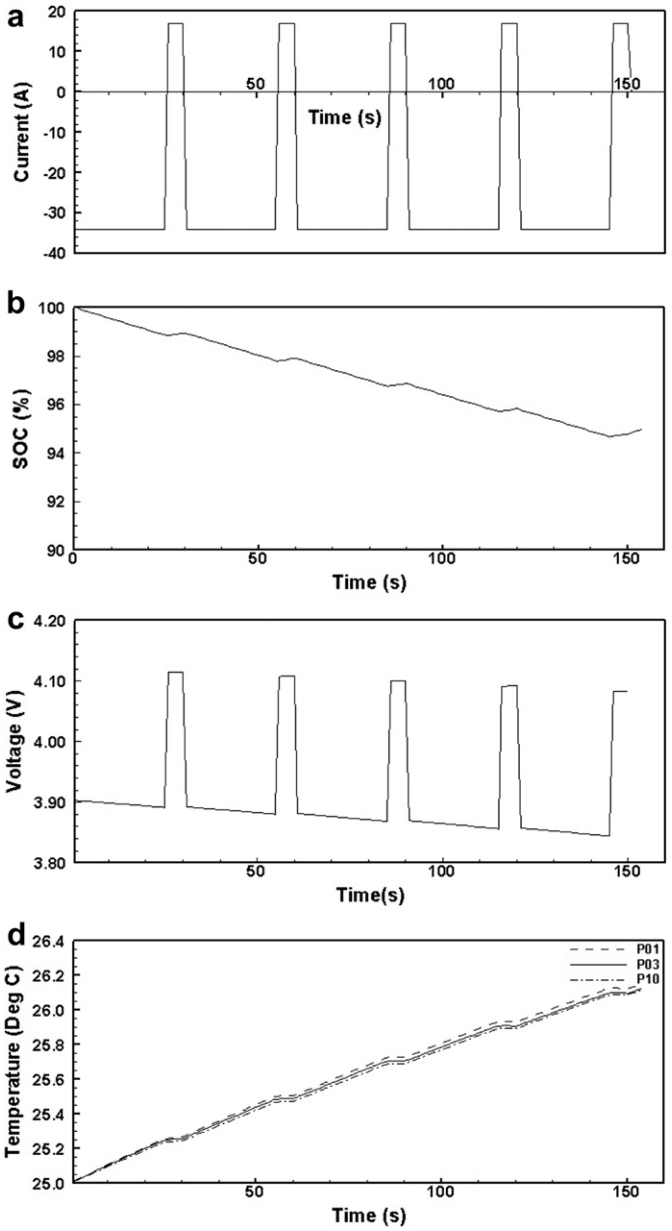

Fig. 8. Electro-thermal model prediction for a severe electric vehicle operating condition (Cycle B). a) Current, b) SOC, c) average voltage, and d) temperatures at P01, P03 and P10.

5. Conclusions

A three-dimensional electro-thermal cell model is developed for predicting the electrical and thermal behaviour of a Li-ion polymer cell. The fully coupled model has been implemented based on a finite volume method. The DOD dependency of the cell is characterised using the experimental test data. The Li-ion cell test data were utilised to validate the electro-thermal model. The electro-thermal model predicts the cell temperature and voltage magnitudes accurately for the test load cycle. The electro-thermal model is then used to predict the cell-level performance for two different vehicle drive cycles: one for a mild EV operating condition, and the other for a more severe operating condition. It is found that a significant temperature rise occurs during the severe drive cycle, and an effective temperature control is required to maintain the optimal cell performance. The model has shown the potential to be used in battery thermal management studies for EV/HEV applications. The electro-thermal data and insights on cell surface temperature variation would aid better design of battery thermal management systems. In a separate study, the proposed electro-thermal cell model is being implemented to predict cell thermal performance estimations in battery management system and vehicle drive cycle modelling applications. The current work is also being extended to model the cell electrical dynamics and their effect on the voltage and temperature.

Acknowledgments

The authors would like to thank the Vehicle Integration group at Tata Motors European Technical Centre Plc and the Low Carbon Vehicle Technology Project (LCVTP). The Low Carbon Vehicle Technology Project (LCVTP) is a collaborative research project between leading automotive companies and research partners, revolutionising the way vehicles are powered and manufactured. The project partners include Jaguar Land Rover, Tata Motors European Technical Centre, Ricardo, MIRA LTD., Zytek, WMG and Coventry University. The project includes 15 automotive technology development work-streams that will deliver technological and socio-economic outputs that will benefit the West Midlands Region, UK. This project is funded by Advantage West Midlands (AWM), UK and the European Regional Development Fund (ERDF).

References

[1] T.M. Bandhauer, S. Garimella, T.F. Fuller, Journal of Electrochemical Society 158 (3) (2011) R1–R25.
[2] S. Chacko and S. Charmer. Concept development and CAE for EV battery thermal management. In IMechE Conference VTMS10, pages C1305–028, Gaydon, UK, 2011.
[3] R. Kizilel, R. Sabbah, J.R. Selman, S. Al-Hallaj, Journal of Power Sources 194 (2) (2009) 1105–1112.
[4] C.G. Motloch, J.P. Christophersen, J.R. Belt, R.B. Wright, G.L. Hunt, R.A. Sutula, T.Q. Duong, T.J. Tartamella, H.J. Haskins, T.J. Miller, High-Power Battery Testing Procedures and Analytical Methodologies For HEV's, SAE International, 2002, 2002-01-1950.
[5] C.-W. Park, A.K. Jaura, Dynamic Thermal Model of Li-Ion Battery for Predictive Behavior in Hybrid and Fuel Cell Vehicles, SAE International, 2003, 2003-01-2286.
[6] R. Mahamud, C. Park, Journal of Power Sources 196 (2011) 5685–5696.
[7] J.-P. Semerie. Lithium-ion batteries for geosynchronous satellites. Qualification test results of the STENTOR battery. In 35th Intersociety Energy Conversion Engineering Conference and Exhibit, volume 1, pages 621–628, 24–28 July, Las Vegas, NV, USA, 2000.

[8] B. V. Ratnakumar, M. C. Smart, G. Halpert, A. Kindler, H. Frank, S. Di Stefano, R. Ewell, and S. Surampudi. Lithium batteries on 2003 Mars Rover. In 17th Annual Battery Conference on Applications and Advances, pages 47–51, 15-18 January, 2002.
[9] J. Yamaki, M. Ihara, and S. Okada. Improvement of thermal stability of lithium ion batteries by using methyl difluoroacetate as an electrolyte solvent. In 25th Annual International Telecommunications Energy Conference, pages 59–65, 19-23 October, 2003.
[10] J. Nguyen and C. Taylor. Safety performance for phosphate based large format lithium-ion battery. In 26th Annual International Telecommunications Energy Conference, pages 146–148, 2004.
[11] A. A. Pesaran and M. Keyser. Thermal characteristics of selected EV and HEV batteries. In 16th Annual Battery Conference on Applications and Advances, pages 219–225, Hawaii, USA, 2001.
[12] A. A. Pesaran, A. Vlahinos, and T. Stuart. Cooling and preheating of batteries in hybrid electric vehicles. In 6th ASME-JSME Thermal Engineering Conference, Hawaii, USA, 2003.
[13] U.S. Kim, J. Yi, C.B. Shin, T. Han, S. Park, Journal of Power Sources 196 (11) (2011) 5115–5121.
[14] K.H. Kwon, C.B. Shin, T.H. Kang, C.-S. Kim, Journal of Power Sources 163 (1) (2006) 151–157.
[15] J. Newman, W. Tiedemann, Journal of Electrochemical Society 140 (7) (1993) 1961–1968.
[16] C.Y. Wang, V. Srinivasan, Journal of Power Sources 110 (2) (2002) 364–376.
[17] D. Bernardi, E. Pawlikowski, J. Newman, Journal of Electrochemical Society 132 (1) (1985) 5–12.
[18] U.S. Kim, C.B. Shin, C.-S. Kim, Journal of Power Sources 180 (2) (2009) 909–916.
[19] L. Rao, J. Newman, Journal of Electrochemical Society 144 (8) (1997) 2697–2704.
[20] W.B. Gu, C.Y. Wang, Journal of Electrochemical Society 147 (2000) 2910–2922.
[21] S.C. Chen, C.C. Wan, Y.Y. Wang, Journal of Power Sources 140 (2005) 111–124.
[22] H. Gu, Journal of Electrochemical Society 130 (1983) 1459–1464.
[23] K. Smith, C.-Y. Wang, Journal of Power Sources 160 (2006) 662–673.
[24] Tata Motors European Technical Centre (TMETC). Hot environment test. Internal and confidential report, 2011.